Theoretical Study of Oxidative Addition and Reductive Elimination of 14-Electron d^{10} ML$_2$ Complexes: A ML$_2$ + CH$_4$ (M = Pd, Pt; L = CO, PH$_3$, L$_2$ = PH$'_2$CH$_2$CH$_2$PH$_2$) Case Study

**Ming-Der Su* and San-Yan Chu***

Department of Chemistry, National Tsing Hua University, Hsinchu 30043, Taiwan, R.O.C.

Received March 18, 1997

We have chosen six ML$_2$ complexes, with a systematic variation in the ligands and metals, to investigate oxidative additions as well as reductive eliminations by using the MP2/LANL2DZ and the MP4SDTQ//MP2/LANL2DZ levels of theory. A qualitative model based on the theory of Pross and Shaik (Su, M.-D. *Inorg. Chem.* **1995**, *34*, 3829) has been used to develop an explanation for the barrier heights. Considering the geometrical effect, the substituent effect, and the nature of the metal center, the following conclusions emerge: for 14-electron ML$_2$ complexes, a smaller L−M−L angle and a better electron-donating ligand as well as a heavier transition metal center (such as Pt) should be a potential model for the oxidative addition of saturated C−H bonds. Conversely, a linear structure and a better electron-withdrawing ligand as well as a lighter transition metal center (such as Pd) would be a good candidate for reductive coupling of C−H bonds. The results obtained are in good agreement with the available experimental results and permit a number of predictions to be made.

I. Introduction

Oxidative addition and reductive elimination are crucial steps in many homogeneous catalytic processes. Hence, an understanding of the factors that influence the mechanisms, rates, and reactivity patterns associated with alkane activation as well as elimination reactions has been recognized as an important and challenging objective by organometallic chemists for at least three decades. Experimental progress in this area has been extensively reviewed.[1] The first report of direct reaction between a soluble Pt(0) complex and a variety of alkanes appeared.[2] Through the elegant studies performed by Whitesides and co-workers, it was found that alkanes can be activated by an intermediate via the thermal reductive elimination of neopentane from *cis*-hydridoneopentyl[bis(dicyclohexylphosphino)ethane]platinum(II) (see **1** in eq 1). Although this intermediate, which is proposed to be [bis(dicyclohexylphosphino)ethane]platinum(0) (**2**), has not been identified directly, its structure and presence are strongly supported by the characterization of the alkyl, aryl, and olefin platinum complexes that are obtained from its many reactions. Whitesides et al. attributed the much higher reactivity of **2** with respect to intermolecular C−H bond activation relative to other linear ML$_2$ intermediates to the bent P−Pt−P conformation dictated by the

$$\text{(1)}$$
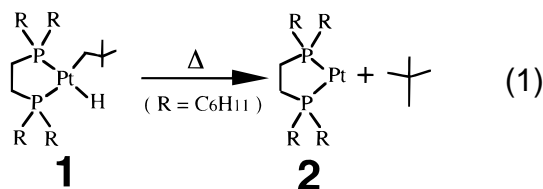
chelating ligand.[2a,b] As suggested by Whitesides et al., this can be explained on the basis of conventional molecular orbital (MO) theory.[3] In a linear L$_2$Pt^0 complex, the HOMO (see details below) is sheltered between the two ligands, whereas in the bent [bis(phosphine)]platinum(0) species, the HOMO extends into space, apparently more appropriately oriented for oxidative addition of C−H bonds. Similar experimental evidence and conclusions can also be found in Otsuka's work.[4] Nevertheless, we believe that a somewhat different approach and emphasis on other aspects of the reaction analyzed here may supplement this general belief.

In this study, we thus report the results of an ab initio MO study of the oxidative addition of methane to 14-electron d^{10} ML$_2$ complex: CH$_4$ + ML$_2$ (M = Pd, Pt), in which L groups (CO, PH$_3$, H$_2$PCH$_2$CH$_2$PH$_2$) have the basic electronic effects of those ancillary ligands that are usually found in general organometallic compounds. It will be shown that the reaction activity of the 14-electron d^{10} ML$_2$ complex is correlated strongly to its singlet−triplet splitting.

II. Origin of the Barrier for Oxidative Addition of ML$_2$

To highlight the questions which formed the basis for our study, it is, perhaps, worthwhile to review briefly the electronic structures of the ML$_2$ fragment. The orbitals of the ML$_2$ fragment are known and have been studied extensively by

(1) For reviews, see: (a) Parshall, G. W. *Acc. Chem. Res.* **1975**, *8*, 113. (b) Hill, C. L. *Activation and Functionalization of Alkanes*; Wiley: New York, 1989. (c) Halpern, J. *Inorg. Chim. Acta* **1985**, *100*, 41. (d) Ephritikhine, M. *New J. Chem.* **1986**, *10*, 9. (e) Jones, W. D.; Feher, F. J. *Acc. Chem. Res.* **1989**, *22*, 91. (f) Ryabov, A. D. *Chem. Rev.* **1990**, *90*, 403. (g) Davies, J. A.; Watson, P. L.; Liebman, J. F.; Greenberg, A. *Selective Hydrocarbon Activation, Principles and Progress*; VCH Publishers Inc.: New York, 1990. (h) Bergman, R. G. *Adv. Chem. Ser.* **1992**, *230*, 211. (i) Crabtree, R. H. *Angew. Chem., Int. Ed. Engl.* **1993**, *32*, 789. (j) Schroder, D.; Schwarz, H. *Angew. Chem., Int. Ed. Engl.* **1995**, *34*, 1937. (k) Amdtsen, B. A.; Bergman, R. G.; Mobley, T. A.; Peterson, T. H. *Acc. Chem. Res.* **1995**, *28*, 154. (l) Siegbahn, P. E. M. *J. Am. Chem. Soc.* **1996**, *118*, 1487.

(2) (a) Hackett, M.; Ibers, J. A.; Jernakoff, P.; Whitesides, G. M. *J. Am. Chem. Soc.* **1986**, *108*, 8094. (b) Hackett, M.; Whitesides, G. M. *J. Am. Chem. Soc.* **1988**, *110*, 1449. (c) Hackett, M.; Ibers, J. A.; Whitesides, G. M. *J. Am. Chem. Soc.* **1988**, *110*, 1436.

(3) Albright, T. A.; Burdett, J. K.; Whangbo, M.-H. *Orbital Interactions in Chemistry*, John Wiley & Sons: New York, 1985.

(4) (a) Otsuka, S. *J. Organomet. Chem.* **1980**, *200*, 191. (b) Yoshida, T.; Tatsumi, K.; Otsuka, S. *Pure Appl. Chem.* **1980**, *52*, 713.
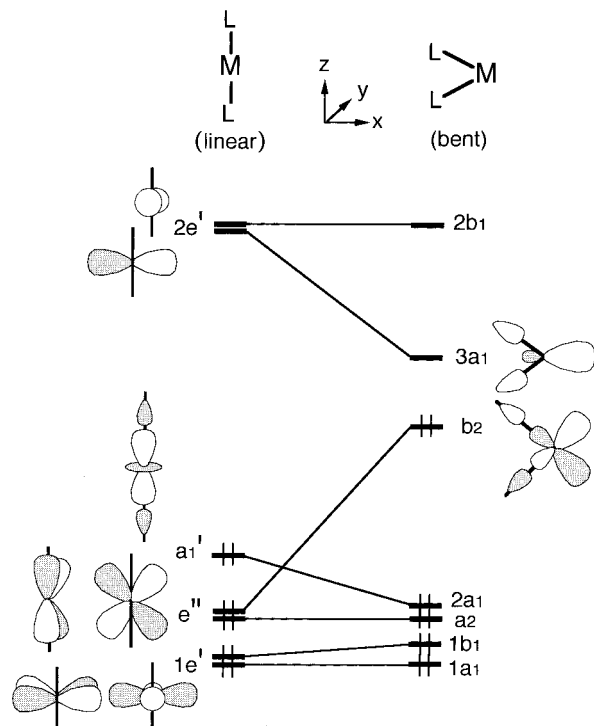
Figure 1. Orbital correlation diagram for 14-electron d^{10} ML$_2$ complexes in bent (right) as well as linear geometries.

Hoffmann et al.,[5] Burdett,[6] Low and Goddard,[7] and Ziegler[8] using different approaches. Figure 1 shows a qualitative Walsh diagram for changing the L−M−L angle.

Hence, the geometrical implications of Figure 1 are clear. A low-spin d^{10} complex, configuration $(1e')^4(e'')^4(a_1')^2$, prefers a linear structure in terms of the Walsh diagram, which has been confirmed by some experimental observations.[9] However, in a bent geometry, the HOMO (b$_2$) is stabilized as the L−M−L angle increases and the LUMO (3a$_1$) increases in energy, resulting in an opening of a HOMO−LUMO gap in the linear d^{10} ML$_2$ complex. Therefore, based on this orbital rationale, it is expected that *the triplet state of the d^{10} ML$_2$ system should be more bent than its singlet analogue.*[10] Moreover, the energy gap between the HOMO and LUMO levels for the d^{10} ML$_2$ species is strongly dependent on the L−M−L angle, as shown in Figure 1, i.e., *the smaller the bond angle (L−M−L), the smaller the singlet−triplet splitting ($\Delta E_{st} = E_{triplet} - E_{singlet}$) of the d^{10} ML$_2$ complex* (vide infra).

Furthermore, since CH$_2$ and 14-electron ML$_2$ are isolobal,[11] each should have two valence orbitals with the same symmetry properties (for ML$_2$, see Figure 1). These are shown in **3**, in which each fragment has one orbital of a$_1$ and b$_2$ symmetry.


3
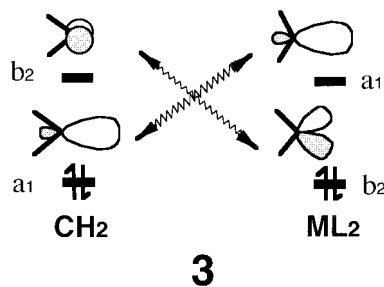
It has to be noted that for methylene, the a$_1$ orbital is lower in energy than the b$_2$ orbital, whereas for ML$_2$ species, b$_2$ lies lower than a$_1$. This is a natural consequence of the fact that, in ML$_2$, the major contribution to the b$_2$ orbital is the metal d character, while in the a$_1$ orbital it is mainly the metal s and p characters.[3] Therefore, for a singlet CH$_2$ fragment, one would assign the two electrons to the a$_1$ orbital, while for a singlet 14-electron ML$_2$ species, the two electrons would go into the b$_2$ level. In other words, the frontier orbitals of the 14-electron ML$_2$ complex consist of an empty s/p hybrid orbital and an "in-L−M−L-plane" d orbital that has a single lone pair of electrons.

As mentioned in the Introduction, the traditional explanation for such higher activity of the bent ML$_2$ complex (such as **2** in eq 1) is attributed to its constrained geometry resulting in a hybridized HOMO (see b$_2$ in Figure 1) that points away from the two attached ligands in order to lead to a better overlap with the incoming CH$_4$ molecule. Nevertheless, we shall use a simple valence-bond model that may supplement this conventional belief and help us understand the origin of barrier height. According to Su's work,[12a] which is based on the theory of Pross and Shaik,[13] it was suggested that the singlet−triplet splitting of carbene plays a crucial role in insertion reactions, i.e., the relative stabilities of the lowest singlet and triplet states are, in turn, a sensitive function of the barrier height for carbenic reactivity. Since, as mentioned above, 14-electron ML$_2$ is isolobal to CH$_2$:[11] one may envision that these predictions for carbenic reactivity should also apply to the 14-electron ML$_2$ systems. We therefore take the oxidative addition reaction ML$_2$ + CH$_4$ as an example by using the configuration mixing (CM) model, as shown in Figure 2, to reveal the origin of barrier height and bonding nature of the ML$_2$ species.

Basically, the oxidative addition reaction may exist in a number of predetermined states, each of which may be approximated by the appropriate molecular orbital configuration. However, as shown in Figure 2, there are only two predominant configurations that contribute considerably to the total wave function Ψ and, in turn, affect the shape of the potential energy surface. One is ϕ_1, which describes the reactant molecule in the ground state but an excited configuration in the product region. The other is ϕ_2, which represents an excited reactant configuration but is the predominant descriptor of the products in their ground state. It is notable that the product configuration (ϕ_2) which arises from the excitation of ML$_2$ and CH'H$_3$ to the

(5) Tatsumi, K.; Hoffmann, R.; Yamamoto, A.; Stille, J. K. *Bull. Chem. Soc. Jpn.* **1981**, *54*, 1857.

(6) (a) Burdett, J. K. *J. Chem. Soc., Faraday Trans. 2* **1974**, *70*, 1599. (b) Burdett, J. K. *Molecular Shapes*; Wiley-Interscience: New York, 1980.

(7) (a) Low, J. J.; Goddard, W. A., III. *J. Am. Chem. Soc.* **1984**, *106*, 6928. (b) Low, J. J.; Goddard, W. A., III. *J. Am. Chem. Soc.* **1984**, *106*, 8321. (c) Low, J. J.; Goddard, W. A., III. *Organometallics* **1986**, *5*, 609.

(8) (a) Ziegler, T. *Inorg. Chem.* **1985**, *24*, 1547. (b) Li, J.; Schreckenbach, G.; Ziegler, T. *Inorg. Chem.* **1995**, *34*, 3245.

(9) (a) Davies, B.; McNeish, M.; Poliakoff, M.; Turner, J. J. *J. Am. Chem. Soc.* **1977**, *99*, 7573. (b) Burdett, J. K. *Coord. Chem. Rev.* **1978**, *27*, 1. (c) Poliakoff, M.; Turner, J. J. *J. Chem. Soc., Dalton Trans.* **1974**, 2276.

(10) This prediction is also supported by Low and Goddard's work; see ref 7a.

(11) Hoffmann, R. *Angew. Chem., Int. Ed. Engl.* **1982**, *21*, 711.

(12) (a) Su, M.-D. *Inorg. Chem.* **1995**, *34*, 3829. (b) Su, M.-D.; Chu, S.-Y. *Organometallics* **1997**, *16*, 1621. (c) Su, M.-D.; Chu, S.-Y. *J. Am. Chem. Soc.* **1997**, *119*, 5373. (d) Su, M.-D.; Chu, S.-Y. *J. Phys. Chem.* **1997**, *101*, 6798. (e) Su, M.-D.; Chu, S.-Y. *J. Am. Chem. Soc.* **1997**, *119*, 10178.

(13) (a) Pross, A.; Shaik, S. *Acc. Chem. Res.* **1983**, *16*, 363. (b) Pross, A. *Adv. Phys. Org. Chem.* **1985**, *21*, 99. (c) Shaik, S. *Prog. Phys. Org. Chem.* **1985**, *15*, 197. (d) Shaik, S.; Schlegel, H. B.; Wolfe, S. *Theoretical Aspects of Physical Organic Chemistry*; John Wiley & Sons Inc.: New York, 1992. (e) Shaik, S.; Hiberty, P. C. *Adv. Quantum Chem.* **1995**, *26*, 99.
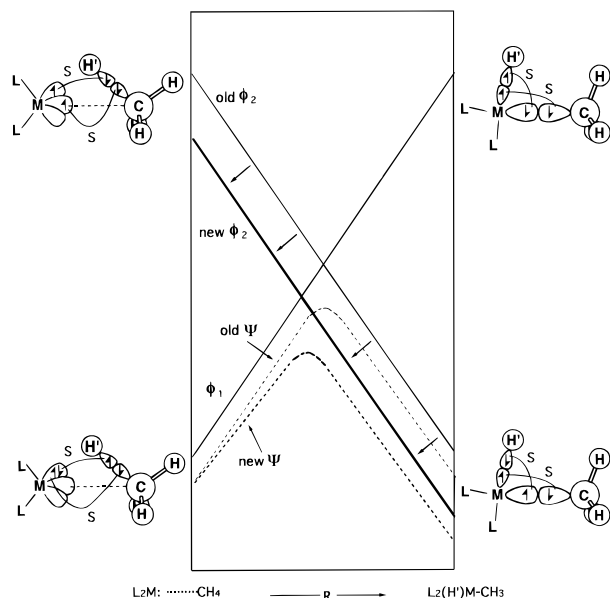
Figure 2. Energy diagram for an oxidative addition reaction showing the formation of a state curve (Ψ) by mixing two configurations: the reactant configuration (ϕ_1) and the product configuration (ϕ_2). S stands for singlet. This energy diagram also shows the effects of stabilizing the product configuration ϕ_2 (indicated by the arrows).

ditriplet (overall singlet) state allows both M–H and M–C bond formation and simultaneous C–H′ bond breaking. There are, of course, other intermediate configurations with different spin states that might contribute to the total wave function Ψ. But since we are only concerned with singlet states in the course of the reaction, it can be assumed that those intermediate configurations contribute very little, if at all, to Ψ and can, therefore, be neglected. Consequently, the reaction mechanism, in a qualitative manner, will be governed by the nature of the configurations from which the profile is built up, and the character of the transition state will reflect the extent to which the configurations mix into its wave function. Moreover, since the barrier height is basically governed by the avoided crossing of the configuration ϕ_1 and ϕ_2, it is readily apparent that a $\phi_1 \rightarrow \phi_2$ excitation will correlate with the barrier, i.e., both ΔE_{st} ($= E_{triplet} - E_{singlet}$ for ML$_2$) and $\Delta E_{\sigma\sigma^*}$ ($= E_{triplet} - E_{singlet}$ for CH$_4$). Accordingly, if a factor is introduced into the system which has the effect of stabilizing ϕ_2, then ϕ_2 will be displaced to a lower energy along the entire reaction coordinate (see Figure 2).[12,13] The effect of such a perturbation is predicted (1) to reduce the reaction barrier since the intended crossing of ϕ_1 and ϕ_2 is lower in energy, (2) to produce a larger exothermicity since the energy of the product is now lower than that of the reactant, and (3) to lead to an earlier transition state since the intended crossing point is now earlier along the reaction coordinate. It should be mentioned here that the predictions from the CM model are basically in accordance with Hammond's postulate.[14] From this analysis, one may easily anticipate that, if $\Delta E_{\sigma\sigma^*}$ is a constant, then a smaller value of ΔE_{st} leads to a lower barrier height and a larger exothermicity, i.e., a linear relationship between ΔE_{st} and the activation energy as well as enthalpy is expected. We shall see calculational results supporting this prediction below.

III. Computational Methods

Geometries of reactants, precursor complexes, transition states, and products were fully optimized by employing the second-order Møller–

(14) Hammond, G. S. *J. Am. Chem. Soc.* **1954**, *77*, 334.

Plesset (MP2) perturbation theory without imposing any symmetry constraints. All electrons, for which the MOs are described by basis functions, were correlated. For triplet ML$_2$ systems, we also carried out second-order unrestricted MP calculations (UMP2) with annihilation of the spin contaminants (PUMP2).[15]

Effective core potentials (ECPs) were used to represent the 28 and 60 innermost electrons of the palladium (up to the 3d shell) and platinum (up to the 4f shell) atoms,[16] respectively, as well as the 10-electron core of the phosphorus atom.[17] For these atoms, the basis set was that associated with the pseudopotential,[16,17] with a standard LANL2DZ contraction.[18] For hydrogen and carbon atoms, the double-ζ basis of Dunning–Huzinaga was used.[19] Hence, the MP2 calculation is denoted by MP2/LANL2DZ.

Vibrational frequencies at stationary points were calculated at the MP2/LANL2DZ level of theory to identify them as minima (zero imaginary frequencies) or transition states (one imaginary frequency). We used these frequencies to evaluate the corresponding zero-point vibrational energy (ZPE/MP2/LANL2DZ) corrections to the total energies.

For better energetics, single-point calculations with MP2/LANL2DZ geometries were carried out at a higher level of theory, the fourth-order MP level, including single, double, triple, and quadruple configurations (MP4SDTQ), using the same basis sets as mentioned above, MP4SDTQ//MP2/LANL2DZ. In addition, the total energies at the highest level were estimated by adding the correction for zero-point energies (ZPE/MP2/LANL2DZ) to the MP4SDTQ energies. Moreover, for triplet ML$_2$, the spin-projected MP perturbation theory to the fourth order (PMP4) with the LANL2DZ basis set was used.[15] All calculations were performed with the Gaussian 94 program.[18]

IV. Results and Discussion

The optimized geometries of the reactants, precursor complexes, transition states, and products for ML$_2$ (M = Pd, Pt; L = CO, PH$_3$; L$_2$ = H$_2$PCH$_2$CH$_2$PH$_2$) at the MP2/LANL2DZ level are given in Figures 3–5. Their energy parameters, calculated at the MP2/LANL2DZ and MP4SDTQ//MP2/LANL2DZ levels, are listed in Table 1. The potential energy profiles at the MP4SDTQ level are, therefore, summarized in Figure 6.

Several important conclusions can be drawn from Figure 6 and Table 1. First, as shown in Table 1, in the first step the reactants yield a precursor complex with a stabilization energy of 1.11, 0.70, 3.49, and 5.31 kcal/mol at the MP2 level and 4.27, 2.01, 4.58, and 5.84 kcal/mol at the MP4SDTQ level for Pd(CO)$_2$, Pt(CO)$_2$, Pd(H$_2$PCH$_2$CH$_2$PH$_2$), and Pt(H$_2$PCH$_2$CH$_2$-PH$_2$), respectively. In the Pd(PH$_3$)$_2$ and Pt(PH$_3$)$_2$ cases, the energy of the precursor complex is, however, higher than that of the corresponding reactants by 2.50, 2.39 kcal/mol at the MP2 level and 2.06, 2.05 kcal/mol at the MP4SDTQ level, respectively. We have examined carefully the energy change along the metal–carbon distance. It is interesting to note that only the precursor complex of Pd(PH$_3$)$_2$ and Pt(PH$_3$)$_2$ adopts the η^1-H geometry. That is, CH$_4$ is bound in an end-on fashion through one hydrogen atom, while in the other cases CH$_4$ does not approach metal in this way. In any event, it is reasonable

(15) (a) Sosa, C.; Schlegel, H. B. *J. Am. Chem. Soc.* **1987**, *109*, 4193. (b) Sosa, C.; Schlegel, H. B. *J. Am. Chem. Soc.* **1987**, *109*, 7007.
(16) Hay, J. P.; Wadt, W. R. *J. Chem. Phys.* **1985**, *82*, 299.
(17) Hay, J. P.; Wadt, W. R. *J. Chem. Phys.* **1985**, *82*, 284.
(18) Frisch, M. J.; Trucks, G. W.; Schlegel, H. B.; Gill, P. M. W.; Johnson, B. G.; Robb, M. A.; Cheeseman, J. R.; Keith, T.; Petersson, G. A.; Montgomery, J. A.; Raghavachari, K.; Al-Laham, M. A.; Zakrzewski, V. G.; Ortiz, J. V.; Foresman, J. B.; Cioslowski, J.; Stefanov, B. B.; Nanayakkara, A.; Challacombe, M.; Peng, C. Y.; Ayala, P. Y.; Chen, W.; Wong, M. W.; Andres, J. L.; Replogle, E. S.; Gomperts, R.; Martin, R. L.; Fox, D. J.; Binkley, J. S.; Defrees, D. J.; Baker, J.; Stewart, J. P.; Head-Gordon, M.; Gonzalez, C.; Pople, J. A. *Gaussian 94*, Revision B.2; Gaussian, Inc.: Pittsburgh, PA, 1995.
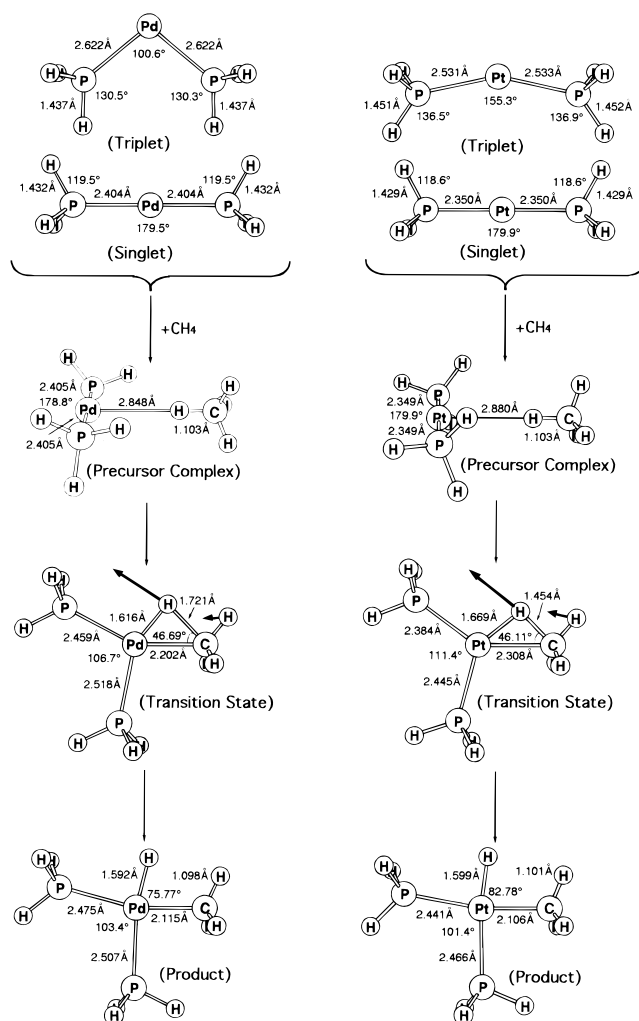(19) Dunning, T. H.; Hay, P. J. In *Modern Theoretical Chemistry*; Schaefer, H. F., Ed.; Plenum: New York, 1976; pp 1–28.
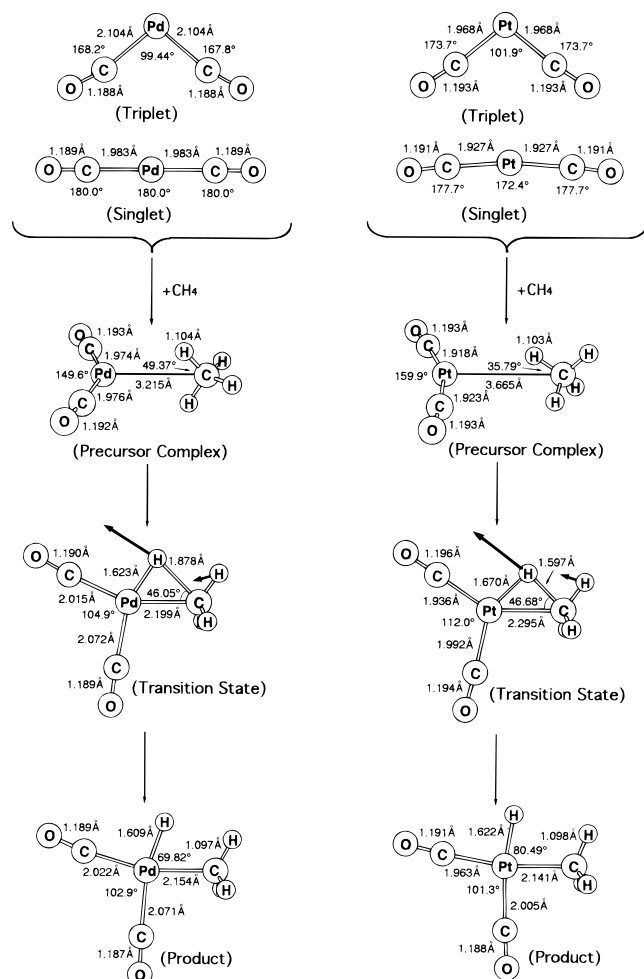
Figure 3. MP2/LANL2DZ optimized geometries at reactants (singlet and triplet), precursor complexes, transition states, and products of Pd(CO)$_2$ and Pt(CO)$_2$. The heavy arrows indicate transition vectors for the single imaginary frequency.

Figure 4. MP2/LANL2DZ optimized geometries at reactants (singlet and triplet), precursor complexes, transition states, and products of Pd(PH$_3$)$_2$ and Pt(PH$_3$)$_2$. The heavy arrows indicate transition vectors for the single imaginary frequency.

to conclude from these data that, for Pd(PH$_3$)$_2$ and Pt(PH$_3$)$_2$ systems, a precursor complex might not exist in the course of the reaction based on our calculations presented here.

Second, considering the geometrical effect, our theoretical findings suggest that, from a kinetic viewpoint, the oxidative addition reactions of bent ML$_2$ systems dictated by the chelating ligand are more facile than those of linear ML$_2$ species. For example, the activation energies at the MP4SDTQ//MP2/LANL2DZ level for oxidative addition of Pt(H$_2$PCH$_2$CH$_2$PH$_2$) and Pd(H$_2$PCH$_2$CH$_2$PH$_2$) were calculated to be 0.75 and 15.2 kcal/mol, respectively, which are quite small relative to the other barriers for linear ML$_2$ systems. Our model calculations are consistent with some experimental findings.[2,4]

Third, considering the substituent effect, it is apparent that the more strongly electron-donating the ligand L, the lower the activation energy for oxidative addition (left to right in Figure 6), but also the higher the heat of reductive elimination (right to left in Figure 6). For instance, at the MP4 level of theory, since the electron-donating ability is in the order M(H$_2$PCH$_2$-CH$_2$PH$_2$) > M(PH$_3$)$_2$ > M(CO)$_2$,[20] the barrier height for CH$_4$

activation with the Pd metal increases in the order Pd(H$_2$PCH$_2$-CH$_2$PH$_2$) (15.1 kcal/mol) < Pd(PH$_3$)$_2$ (29.2 kcal/mol) < Pd(CO)$_2$ (32.9 kcal/mol), and for the Pt metal Pt(H$_2$PCH$_2$CH$_2$-PH$_2$) (0.749 kcal/mol) < Pt(CO)$_2$ (25.7 kcal/mol) < Pt(PH$_3$)$_2$ (26.5 kcal/mol),[21] while the activation energy for CH$_4$ elimination decreases in the order Pd(H$_2$PCH$_2$CH$_2$PH$_2$) (−1.34 kcal/mol) > Pd(PH$_3$)$_2$ (−1.45 kcal/mol) > Pd(CO)$_2$ (−4.20 kcal/mol), and Pt(H$_2$PCH$_2$CH$_2$PH$_2$) (16.5 kcal/mol) ~ Pt(PH$_3$)$_2$ (16.5 kcal/mol) > Pt(CO)$_2$ (10.4 kcal/mol).[22] Likewise, the reaction enthalpy for oxidative addition increases in the order Pd(H$_2$-PCH$_2$CH$_2$PH$_2$) (16.5 kcal/mol) < Pd(PH$_3$)$_2$ (30.6 kcal/mol) < Pd(CO)$_2$ (37.1 kcal/mol), and Pt(H$_2$PCH$_2$CH$_2$PH$_2$) (−15.7 kcal/mol) < Pt(PH$_3$)$_2$ (9.81 kcal/mol) < Pt(CO)$_2$ (15.3 kcal/mol). These calculational results are in good agreement with some experimental observations[23] as well as earlier theoretical investigations.[7,24]

(20) According to our MP2/LANL2DZ results, it was found that the electronic charge on the metal of those fragments is Pd(H$_2$PCH$_2$CH$_2$-PH$_2$) (−0.203) < Pd(PH$_3$)$_2$ (−0.175) < Pd(CO)$_2$ (+0.0625), and for the Pt metal Pt(H$_2$PCH$_2$CH$_2$PH$_2$) (−0.197) < Pt(PH$_3$)$_2$ (−0.158) < Pt(CO)$_2$ (+0.643). Thus, our computational evidence clearly shows that the electron-donating ability decreases in the same order as we predicted in the article.

(21) It has to be pointed out that the MP2 calculations show the same reactivity order in both Pd and Pt complexes, while the single-point MP4SDTQ calculations show the reactivity order Pd(CO)$_2$ < Pd(PH$_3$)$_2$ and Pt(CO)$_2$ > Pt(PH$_3$)$_2$; the energy difference of the barrier for the latter case is trivial (0.8 kcal/mol). The reason for the variation in the reactivity order on going from MP2 to MP4SDTQ could be that single-point calculations with MP2 geometries were carried out at the MP4SDTQ level in this work. It is therefore believed that using the MP4 level with large basis sets and full geometry optimization should lead to the smaller barrier in both Pd(PH$_3$)$_2$ and Pt(PH$_3$)$_2$.
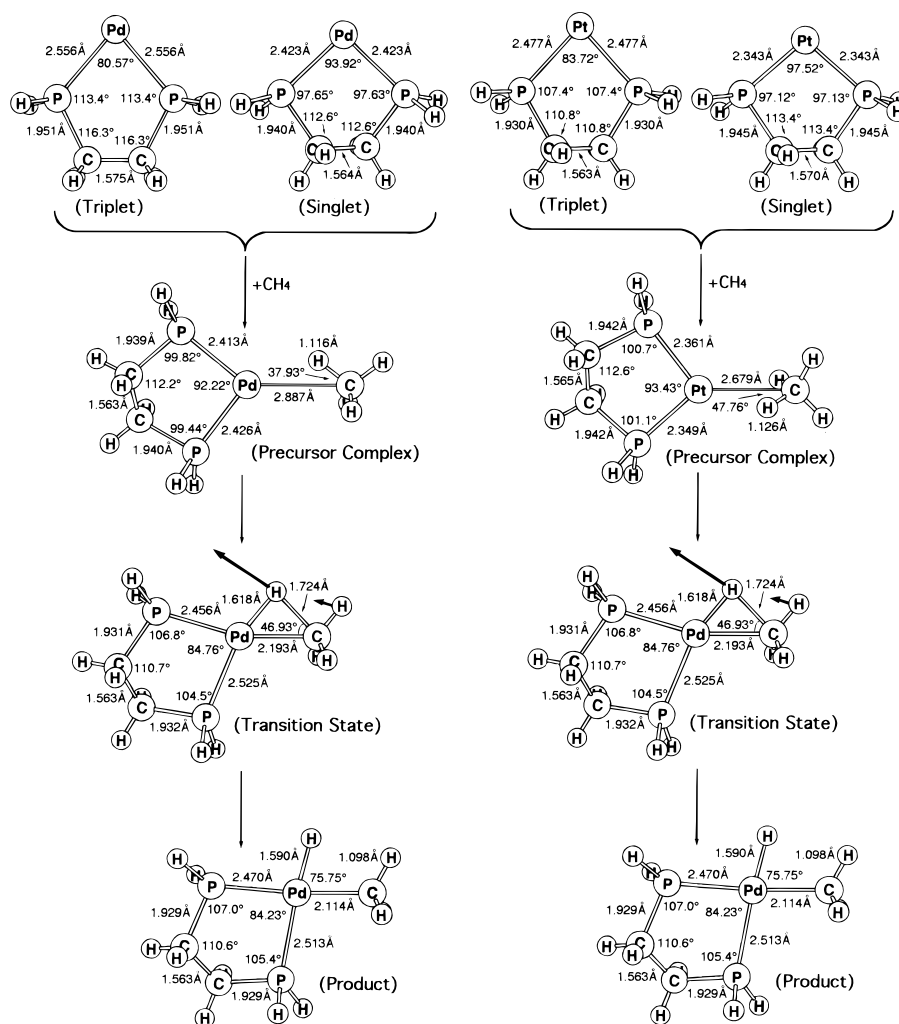
Figure 5. MP2/LANL2DZ optimized geometries at reactants (singlet and triplet), precursor complexes, transition states, and products of Pd(PH$_2$CH$_2$CH$_2$PH$_2$) and Pt(PH$_2$CH$_2$CH$_2$PH$_2$). The heavy arrows indicate transition vectors for the single imaginary frequency.

Fourth, considering the nature of the metal center, it is clear from Table 1 and Figure 6 that the calculated activation energy for oxidative additions is substantially lower for Pt than for Pd, indicating that Pt reaction is more favorable in the activation of the C−H bond. However, the barrier of the Pd systems for the reverse process (i.e., elimination reaction) is quite small relative to the Pt analogues, implying that Pd reaction is more facile in the coupling formation of the C−H bond.[7] These
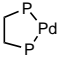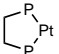
(22) As shown in Table 1, in the case of the Pd series, it was found that the MP2 calculations yield the transition state being more stable than the product, implying that those product optimizations were artificial. Reducing optimization convergence criteria by an order of magnitude still did not change the situation. It appears that the potential energy surfaces for the Pd product complexes are fairly flat. A set of polarization functions on Pd and the ligands and the inclusion of correlation should be essential. This study is, however, beyond the scope of the present work. Nevertheless, our study shows that the single-point MP4 calculations based on the MP2 geometries can provide reliably qualitative conclusions.

(23) (a) Abis, L.; Sen, A.; Halpern, J. *J. Am. Chem. Soc.* **1978**, *100*, 2915. (b) Gillie, A.; Still, J. K. *J. Am. Chem. Soc.* **1980**, *102*, 4933. (c) Halpern, J. *Acc. Chem. Res.* **1982**, *15*, 332. (d) Ozawa, F.; Ito, T.; Nakamura, Y.; Yamamoto, A. *Bull. Chem. Soc. Jpn.* **1981**, *54*, 1868. (e) Whitesides, G. M. *Pure Appl. Chem.* **1981**, *53*, 287. (f) Yoshida, T.; Otsuka, S. *J. Am. Chem. Soc.* **1977**, *99*, 2134. (g) Michelin, R. A.; Faglia, S.; Uguagliati, P. *Inorg. Chem.* **1983**, *22*, 1831.

(24) (a) Kitaura, K.; Obara, S.; Morokuma, K. *J. Am. Chem. Soc.* **1981**, *103*, 2891. (b) Balazs, A. C.; Johnson, K. H.; Whitesides, G. M. *Inorg. Chem.* **1982**, *21*, 2162. (c) Noell, J. O.; Hay, P. J. *J. Am. Chem. Soc.* **1982**, *104*, 4578. (d) Obara, S.; Kitaura, K.; Morokuma, K. *J. Am. Chem. Soc.* **1984**, *106*, 7482.

theoretical findings are in accord with the experimental observation of difficult reductive elimination from Pt complexes.[5,23]

Before further discussion, let us emphasize here the importance of the status of the triplet state for the 14-electron ML$_2$ reactant. Since two new covalent bonds have to be formed in the product ML$_2$(H)(CH$_3$), i.e., the M−H and M−C bonds (right in Figure 2), the bond-prepared ML$_2$ state thus has to have at least two open shells, and the lowest state of this type is the triplet state. Therefore, from the valence-bond point of view, the bonding in the product can be recognized as bonds formed between the triplet ML$_2$ state and the two doublet radicals (overall singlet), the methyl radical, and the hydrogen atom. This is much in the same way as the bonding in the water molecule can be considered as bonds formed between the triplet oxygen atom and the two doublet hydrogen atoms.[11,12] Accordingly, if a reactant ML$_2$ has a singlet ground state with a small excitation energy to the triplet state, this will bring more opportunities for allowing triplet ML$_2$ to take part in the singlet reaction and can readily undergo single-step bond insertions. A plot of activation barrier versus ΔE_{st} (Figure 7) shows that, for the aforementioned six systems, barrier height varies linearly with ΔE_{st} as would be expected: $y = 0.701x - 19.8$ ($x = \Delta E_{st}$, $y =$ the activation energy) at the MP4SDTQ/LANL2DZ level.[25] Likewise, a linear correlation between ΔE_{st} and the reaction

(25) At the MP2/LANL2DZ level, the linear relationship is $y = 0.766x - 21.0$.

Table 1. Energies for Singlet and Triplet ML$_2$ Fragments and for the Process CH$_4$ + ML$_2$ → Precursor Complex → Transition State → Product[a]
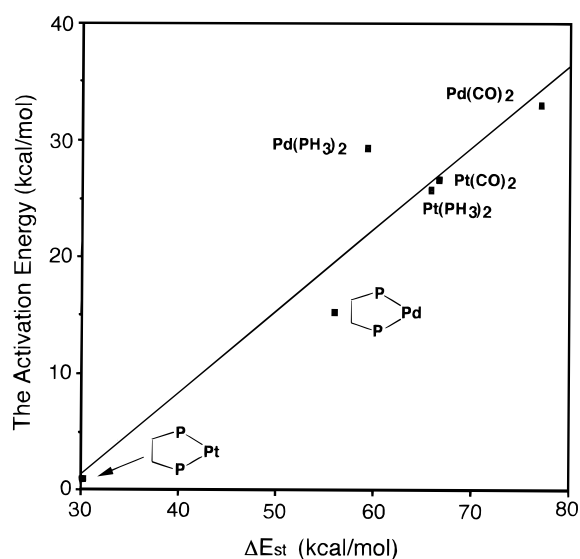
system	singlet (hartrees)	ΔE_{st}[b] (kcal/mol)	reactant[c] (hartrees)	precursor complex[d] (kcal/mol)	transition state[d] (kcal/mol)	product[d] (kcal/mol)
CO−Pd−CO	−351.91989	+77.0	−392.21759	−4.27	+32.9	+37.1
	(−351.87522)	(+72.3)	(−392.15438)	(−1.11)	(+34.2)	(+35.7)
CO−Pt−CO	−344.29607	+65.6	−384.59377	−2.01	+25.7	+15.3
	(−344.25498)	(+64.9)	(−384.53413)	(−0.698)	(+27.6)	(+14.1)
PH$_3$−Pd−PH$_3$	−142.27581	+59.3	−182.57351	+2.06	+29.2	+30.6
	(−142.22025)	(+56.5)	(−182.49940)	(+2.50)	(+29.6)	(+28.0)
PH$_3$−Pt−PH$_3$	−134.64468	+67.2	−174.94238	+2.05	+26.5	+9.81
	(−134.58855)	(+64.8)	(−174.86770)	(+2.39)	(+26.8)	(+6.88)
⟨P⟩Pd (chelate)	−219.34458	+52.3	−259.64229	−4.57	+15.1	+16.5
	(−219.26938)	(+48.6)	(−259.54853)	(−3.49)	(+14.5)	(+12.6)
⟨P⟩Pt (chelate)	−211.69712	+29.7	−251.99482	−5.84	+0.749	−15.7
	(−211.61913)	(+26.0)	(−251.89828)	(−5.31)	(−1.20)	(−21.5)

^{a} At the MP4SDTQ//MP2/LANL2DZ+ZPE and MP2/LANL2DZ+ZPE (in parentheses) levels of theory. See text. ^{b} The energy relative to the corresponding singlet state. A positive value means the singlet is in the ground state. ^{c} The total energies of CH$_4$ at the MP4SDTQ//MP2/LANL2DZ and MP2/LANL2DZ levels are −40.29770 and −40.27915 hartrees, respectively. ^{d} The energy relative to the corresponding reactant. Calculations were performed for a singlet.
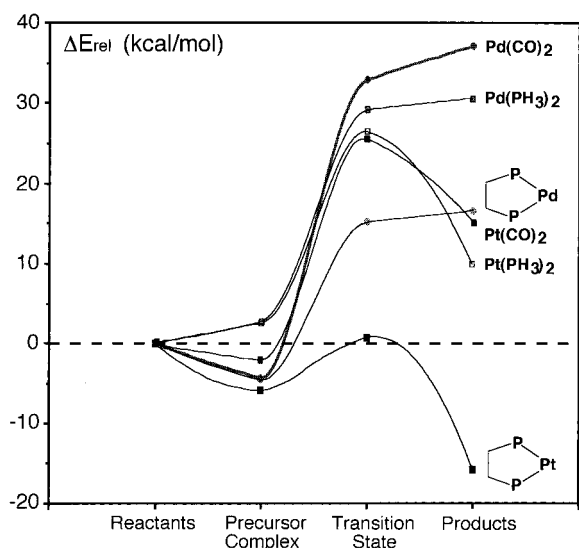
Figure 6. Potential energy profile of the reaction of ML$_2$ with CH$_4$. All of the energies were calculated at the MP4SDTQ//MP2/LANL2DZ+ZPE level (see text).

Figure 7. ΔE_{st} (=$E_{triplet} - E_{singlet}$) for ML$_2$ fragments vs the activation energy for oxidative addition of ML$_2$ fragments to methane. All were calculated at the MP4SDTQ//MP2/LANL2DZ+ZPE level (see the text).

enthalpy (y') is also obtained at the same level of theory: $y' = 0.979x - 42.3$,[26] whose graph is, however, not shown here. These results strongly support the predictions mentioned in the previous section: *The smaller the ΔE_{st} of 14-electron ML$_2$ is, the lower the barrier height is and, in turn, the faster the oxidative addition reaction is, the larger the exothermicity is.* For instance, as shown in Table 1, at the MP4SDTQ level, singlet Pt(CO)$_2$ is more stable than the triplet (ΔE_{st} = 64.9 kcal/mol); thus, ϕ_1 must rise steeply and yields a higher barrier (27.6 kcal/mol) as a result of its crossing with ϕ_2. On the other hand, singlet Pt(H$_2$PCH$_2$CH$_2$PH$_2$), which has a lower ΔE_{st} (26.0 kcal/mol), lies below the triplet, and ϕ_1 rises relatively little before it crosses ϕ_2, resulting in a smaller barrier (−1.20 kcal/mol).

With the above analysis in mind, the reason the bent ML$_2$ favors the oxidative addition can be easily accounted for by the fact that a bent geometry is expected to result in a smaller singlet−triplet energy gap than a linear one due to the MO analysis as discussed earlier. In addition, since sterically bulky substituents favor a large L−M−L bond angle and then enlarge

its singlet−triplet splitting, the steric factor might play a significant role in this reactivity. It is thus suggested that *the ML$_2$ reactant with the bulky groups should hinder the oxidative addition of C−H bonds.* Likewise, one could also predict that *a 14-electron ML$_2$ complex with the strained ring system (such as a chelating bisphosphine as studied in this work), where the L−M−L angle is forced to be less than 180°, would lead to a smaller ΔE_{st} and, in turn, allow a more facile oxidative addition to C−H bonds of alkanes than the linear structure.*

Moreover, considering the substituent effect, our theoretical findings suggest that stronger donor ligands give a lower barrier for the oxidative addition, while better acceptor ligands give a lower barrier for the reductive elimination. The reason for this can be simply understood in terms of the singlet−triplet splitting. Qualitatively, since oxidative addition involves charge transfer from the metal center of ML$_2$ to the incoming methane, the electron-donating L, which can increase the electron density on the central metal, would stabilize its transition state and then lower the barrier height. Additionally, a good π acceptor ligand (such as CO) will stabilize the b$_2$ level of ML$_2$ (see Figure 1) and leave the 3a$_1$ level unchanged. This will increase the HOMO−LUMO gap of ML$_2$ and then enlarge its singlet−triplet

(26) At the MP2/LANL2DZ level, the linear relationship is $y' = 1.03x - 44.8$.

splitting ΔE_{st} ($=E_{triplet} - E_{singlet}$). Such an effect will thus hinder the oxidative addition reaction, as discussed above. On the other hand, since reductive elimination involves charge transfer from methane to metal, the electron-withdrawing L should stabilize the ML_2 complex and then allow such a reaction to proceed readily. Moreover, from another point of view, a better electron donor group L is equivalent to an ancillary ligand with lower electronegativity, while a better electron acceptor group L is equivalent to an ancillary ligand with higher electronegativity. It is therefore anticipated that, *for the 14-electron ML_2 system, the more strongly electron-donating L is or the lower the electronegativity of L is, the more rapid the oxidative addition is; whereas, the more strongly electron-withdrawing L is or the higher the electronegativity of L is, the faster the reductive elimination is.*

Furthermore, since the electron density on the metal center was found to play a fundamental role in determining the reactivity of ML_2, one may expect that the nature of the metal would be responsible for the barrier height in the course of the reaction. Our model calculations have shown that the oxidative addition of PtL_2 has a lower activation energy than that of PdL_2, while the reductive elimination of the former has a higher barrier than that of the latter. The reason for this can be traced back to the singlet−triplet splitting again. It was experimentally reported that the ground state of the Pt atom is triplet s^1d^9 (with the d^{10} state lying at 21.9 kcal/mol, i.e., $\Delta E_{st} = -21.9$ kcal/mol), while that of the Pd atom is singlet d^{10} (with the s^1d^9 state lying at 11.0 kcal/mol, i.e., $\Delta E_{st} = +11.0$ kcal/mol).[27] This strongly indicates that Pt would prefer to remain in the high-spin state, whereas Pd favors the low-spin state. As such, it is reasonably concluded that the promotion energy from the singlet state to the triplet state, used to form the strongest covalent bonds, should be smaller for the Pt complex than for the Pd complex. It is, therefore, predicted that, *for the 14-electron ML_2 cases, the oxidative addition of a third-row transition metal (such as Pt) will be preferable to that of a second-row transition metal (such as Pd), whereas the reductive elimination of a second-row metal will be favorable over that of a third-row homologue.*

Given the importance of the presence of these three effects on the 14-electron ML_2 reactant, one may then foresee that *a smaller L−M−L angle and a better electron-donating ligand as well as a heavier transition metal center (such as the third-row) should be a potential model for the oxidative addition of saturated C−H bonds.* Conversely, *a linear structure and a better electron-withdrawing ligand as well as a lighter transition metal center (such as second-row) would be a good candidate for reductive coupling of C−H bonds.*

In summary, this work represents an attempt to apply the CM model to understand the origin of barriers for the activation of methane by 14-electron ML_2 complexes. In this way, a systematic variation in the ligands and metals has been studied, and their variations with the electronic nature of reactants have been discussed. Although the estimated magnitude of the barrier and the predicted geometry of the transition state for such reactions appear to be dependent on the calculational level applied, our qualitative predictions are in quite good agreement with the calculational results presented here as well as the experimental observations. In particular, our study has shown that the problems concerning the reactivity of oxidative addition as well as reductive elimination for the 14-electron ML_2 systems can be reduced to pictorial considerations. Despite its simplicity, our approach proves to be rather effective and can provide chemists with important insights into the factors controlling the activation of saturated C−H bonds, thus allowing a better understanding of the nature of such systems as well as a number of predictions to be made.[28]

It is hoped that our study will stimulate for further research into the subject.

Note Added in Proof

After this manuscript was submitted, several related papers concerning the mechanism in the activation of C−H bonds by the 14-electron ML_2 complex using quantum chemical methods were published: (1) Sakaki, S.; Biswas B.; Sugimoto, M. *J. Chem. Soc., Dalton Trans*. **1997**, 803. (2) Stromberg, S.; Zetterberg, K.; Siegbahn, P. E. M. *J. Chem. Soc., Dalton Trans.* **1997**, 4147. (3) Sakaki, S.; Biswas, B.; Sugimoto, M. *Organometallics* **1998**, *17*, 1278.

IC970320S

---

(27) Moore, C. E. *Atomic Energy Levels*; National Bureau of Standards: Washington, DC, 1971; Vol. III. (These state splittings were averaged over *j* states to cancel out spin−orbit coupling.)

(28) It must be emphasized that the concept which uses the singlet−triplet splitting ΔE_{st} to predict the reactivity of the 14-electron ML_2 complex cannot apply to the CpCoL system (see ref 1l). Indeed, Siegbahn has pointed out that the cobalt atom has a high excitation energy (77.5 kcal/mol) from a quartet d^7s^2 ground state to the d^9 doublet state, implying that the CpML system has a low amount of open-shell character in the singlet state. In other words, unlike the two main configurations (ϕ_1 and ϕ_2) involved in Figure 2, in the CpCoL case there could be three predominant configurations contributing to the total wave function Ψ, i.e., a closed-shell singlet, two open-shell triplets (so overall singlet), and an open-shell singlet. This study, however, is beyond the scope of the present work and will not be discussed here.